Comparative Biochemistry and Physiology, Part A 203 (2017) 115–125

Contents lists available at ScienceDirect

Comparative Biochemistry and Physiology, Part A

journal homepage: www.elsevier.com/locate/cbpa

Molecular characterization of a cDNA encoding $Na^+/K^+/2Cl^-$ cotransporter in the gill of mud crab (*Scylla paramamosain*) during the molt cycle: Implication of its function in osmoregulation

Bin-peng Xu [a], Dan-dan Tu [a], Mao-cang Yan [b], Miao-an Shu [a,*], Qing-jun Shao [a]

[a] College of Animal Sciences, Zhejiang University, Hangzhou 310058, Zhejiang Province, China
[b] Zhejiang Mariculture Research Institute, Wenzhou 325005, Zhejiang Province, China

ARTICLE INFO

Article history:
Received 20 February 2016
Received in revised form 19 August 2016
Accepted 19 August 2016
Available online 1 September 2016

Keywords:
Decapod crustaceans
Gill structure
Hemolymph
Ion transporters
Molt
Ionoregulation

ABSTRACT

Although iono-regulatory processes are critical for survival of crustaceans during the molt cycle, the mechanisms involved are still not clear. The $Na^+/K^+/2Cl^-$ cotransporter (NKCC), a SLC12A family protein that transports Na^+, K^+ and $2Cl^-$ into cells, is essential for cell ionic and osmotic regulation. To better understand the role of NKCC in the molt osmoregulation, we cloned and characterized a *NKCC* gene from the mud crab, *Scylla paramamosain* (designated as *Sp*NKCC). The predicted *Sp*NKCC protein is well conserved, and phylogenetic analysis revealed that this protein was clustered with crustacean NKCC. Expression of *SpNKCC* was detected in all the tissues examined but was highest in the posterior gills. Transmission electron microscopy revealed that posterior gills had a thick type of epithelium for ion regulation while the anterior gills possessed a thin phenotype related to gas exchange. During the molting cycle, hemolymph osmolality and ion concentrations (Na^+ and Cl^-) increased significantly over the postmolt period, remained stable in the intermolt and premolt stages and then decreased at ecdysis. Meanwhile, the expression of *SpNKCC* mRNA was significantly elevated (26.7 to 338.8-fold) at the ion re-establishing stages (postmolt) as compared with baseline molt level. This pattern was consistent with the coordinated regulation of Na^+/K^+-ATPase α-subunit (*NKA α*), carbonic anhydrase cytoplasmic (*CAc*) isoform and Na^+/H^+ exchanger (*NHE*) genes in the posterior gills. These data suggest that *SpNKCC* may be important in mediating branchial ion uptake during the molt cycle, especially at the postmolt stages.

1. Introduction

Molting, a phenomenon of the periodic shedding the old cuticle and subsequent reconstruction of a new rigid exoskeleton, occurs in all crustaceans and is essential for growth, metamorphosis and reproduction (Ghanawi and Saoud, 2012; Li et al., 2015). Generally, the molt cycle in decapod crustaceans is composed of different stages, including preecdysis (premolt, D stage), ecdysis (E stage), postecdysis (postmolt, A and B stages) and intermolt (C stage) stages (Drach and Tchernigovtzeff, 1967). At ecdysis, the shedding of the restrictive cuticle and the size increase in crustaceans are achieved by the enhanced water absorption (Perry et al., 2001; Wilder et al., 2009). Such increase in water uptake may lead to a simultaneous decrease in hemolymph osmolality and ion concentrations in crustaceans. Hence, osmoregulation is directly affected by the molting process.

Crustaceans do have to keep hemolymph osmolality and major ionic concentrations (Na^+, Cl^-) within the range of physiological homeostasis through absorption and excretion of Na^+ and Cl^- across the gills (Freire et al., 2008; McNamara and Faria, 2012). A suite of ion pumps, ion transporters and ion transport-related proteins in the gills are involved in the active uptake of ions from the external media into the hemolymph. In general, the electrogenic basal Na^+/K^+-ATPase (NKA) drives Na^+ transport to the hemolymph sustained by apical Na^+ uptake possibly through the Na^+/H^+ exchanger (NHE) (Towle et al., 1997a; Chung and Lin, 2006; Leone et al., 2015). The carbonic anhydrase (CA) is believed to provide support for the overall transport mechanisms through the catalyzed hydration of respiratory CO_2, which produces H^+ and HCO_3^- needed to support Na^+/H^+ and HCO_3^-/Cl^- exchange, respectively (Henry, 1988; Serrano and Henry, 2008; McNamara and Faria, 2012). Studies have indicated that $Na^+/K^+/2Cl^-$ cotransporter (NKCC) may also serve as a key ion transporter for marine invertebrates (Riestenpatt et al., 1996; Luquet et al., 2005; Havird et al., 2014).

The $Na^+/K^+/2Cl^-$ cotransporter (NKCC), is a member of the cation-chloride cotransporter (CCC) family that plays an essential role in the osmoregulatory processes in the gills of aquatic species by transporting Na^+, K^+ and Cl^- into animal cells simultaneously (Gagnon et al., 2002; Gamba, 2005). In vertebrates, two distinct isoforms of NKCC cotransporters (NKCC1 and NKCC2) have been identified (Markadieu

* Corresponding author at: Animal Sciences College, Zhejiang University, Zijingang Campus, 866 Yuhangtang Road, Hangzhou 310058, China.
E-mail address: shuma@zju.edu.cn (M. Shu).

http://dx.doi.org/10.1016/j.cbpa.2016.08.019
1095-6433/

Table 1
Primers used in the present study.

Primer name	Sequence 5′→3′	Amplicon size (bp)	Annealing temperature (°C)
SpNKCC-F	TCAACTTCTCCTGYTTCCAC	1029	53
SpNKCC-R	TGCCC TTCTTCTGYTTCCTC		
Universal primer mix (UPM)			
Long primer	CTAATACGACTCACTATAGGGC AAGCAGTGGTATCAACGCAGAGT		
Short primer	CTAATACGACTCACTATAGGGC		
SpNKCC-5′	TGCCTCGCTGTCTGTTCCATCTTG CGTG	2469	68
SpNKCC-3′ outer	TTTCAACACCCTGCATGAGGCTCT GGAC	1093	70
SpNKCC-3′ inner	CAACCAGCTCACGCAAGATGGAA CAGAC	1743	68
SpNKCC real-F	CCTCTGATCTACGCTGGGTG	169	55
SpNKCC real-R	GGACATAACCACGCACAGG		
β-actin real-F	GCCCTTCCTCACGCTATCCT	185	58
β-actin real-R	GCGGCAGTGGTCATCTCCT		
NKA real-F	GGACCTACCACGACCGCAAGATA	113	58
NKA real-R	GGAGTTACGGCGGGTCTTACAAA		
NHE-F	GTGTYTGGGCAAGATTGGBTTCCAC	1630	58
NHE-R	GGCTTGTARTCVTTGGAGAGSAGA		
NHE real-F	GGACAACATCATGGCAGTGGACAT	112	58
NHE real-R	TGGTGACGAAGGCAGTGAGGAA		
CAc-F	CAGGGGTGGTACGACYTGAGTC	633	60
CAc-R	GGGCAGCAAGCAGTCCCCYATTRA		
CAc real-F	GCCGTGCTGGGAATGTTCCTG	120	56
CAc real-R	AAGGAGGCGTGGTGAGAGAGC		
AQP-1-F	TTCGCTGTCGGCATTATTGTC	333	50
AQP-1-R	ACATCGTTGCGTCGCTCGTCA		
AQP-1 real-F	TTCGCTGTCGGCATTATTGTC	185	58
AQP-1 real-R	AGACCCTTCAGGATGGCAGAG		

and Delpire, 2014). In contrast, a unique NKCC has been identified from crustaceans, including *Callinectes sapidus* (Towle et al., 1997b), *Carcinus maenas*, *Chasmagnathus granulatus* (Luquet et al., 2005) and *Halocaridina rubra* (Havird et al., 2014). *NKCC* exhibits a salinity-sensitive expression pattern, and its transcription level increases when crustaceans are exposed to low salinity water (Spanings-Pierrot and Towle, 2004; Luquet et al., 2005; Havird et al., 2014). The NKCC was presumably involved in the initial step of ion transport from the ambient medium to the gill. In the green shore crab *C. maenas*, electrophysiological evidence has been presented for the participation of an apical NKCC in this process (Riestenpatt et al., 1996). Although there is a growing number of evidence implicating the involvement of crustacean NKCC activity in ionic homeostasis in different salinities, very little is known about whether NKCC is involved in osmoregulation during the molt processes in crustaceans. Therefore, the aim of the present study was to gain new insights into the characterization of NKCC and its role in osmoregulation in different molt stages of mud crab (*Scylla paramamosain*), a euryhaline species that was found to molt at least 18 times after metamorphosis (Ong, 1966; Chung and Lin, 2006). Here, we report the molecular cloning of a NKCC from gills of *S. paramamosain*. Further, hemolymph osmolality, ion concentration as well as the mRNA expression patterns of *NKCC*, Na^+/K^+-ATPase α-subunit (*NKA α*), carbonic anhydrase cytoplasmic (*CAc*) isoform, *NHE* and aquaporin-1(*AQP-1*) in the gills of various molt stages were determined. In addition, gill architecture of the intermolt animals has also been studied to assess its possible role as a site for osmoregulation. These findings are brought together to elucidate the biochemical, transcriptional and ultrastructural underpinnings of ion regulation in crustacean during the molt cycle.

2. Materials and methods

2.1. Animal collection and maintenance

The experimental animals, *Scylla paramamosain*, measuring 40.05 ± 6.87 g in weight, were obtained from Wenzhou, Zhejiang Province, China. All individuals were cultured individually in plastic trays (0.3 × 0.2 × 0.2 m) with running seawater of approximately 17 ppt salinity as their original culture water at 29 ± 1 °C. Crabs were fed with live clams every day until 2 days before sampling.

The molt stages were determined by observing the setae on the maxlliped exopodite on the animals under a light microscope (Xu et al., 2015). A and B stages were designated as postmolt stages, C as intermolt, D_0 as early premolt, D_1 as mid premolt, D_2 as late premolt, and E as ecdysis, based on the established criteria (Drach and Tchernigovtzeff, 1967).

2.2. Tissue preparation

Crabs ($n = 7$) in each stage of the molt cycle were sampled. Briefly, hemolymph samples were withdrawn from the infrabranchial sinus at the base of the fifth pereiopod using a 22-gauge needle and 1 mL syringe. The samples were frozen at −20 °C until osmolality determination and ion analysis. For dissection, crabs were anesthetized on crushed ice for 10 min and then anterior (G1), posterior (G6) gills and other tissues (gills, muscle, hepatopancreas, gut, thoracic ganglia, hypodermis, hemocytes, antennal gland and heart) were dissected out and immediately placed in liquid nitrogen and kept at −80 °C until required. Only specimens in the intermolt stage were used for tissue distribution analysis, histological and electron microscopic study.

2.3. Growth metrics

The quantitative method was used as previously described (Chang et al., 2011). At the beginning of the study, crabs (n = 7) from the late premolt stage D_2 were selected and measured individually for carapace parameters (width and length) and weight to the nearest 0.1 mm and 0.01 g, respectively. The crabs were held as described above and the general molting state of these crabs was observed frequently. After ecdysis, carapace parameters and weight of each crab (stage A) were measured within 1 h following the molt stage. The parameters were calculated as follows:

$$\text{Percent weight gain (WG, \%)} = 100\% \times (W_A - W_{LD})/W_{LD}$$

where W_A is the final body weight from early postmolt stage after ecdysis; W_{LD} is the body weight from the late premolt stage.

2.4. Hemolymph osmolality and ion concentrations

Hemolymph samples were thawed on ice, sonicated for 15 s, and centrifuged at 14,000 gravity unit for 1 min to separate out clot material. Osmolality was then measured on 10 μL samples using a vapor pressure osmometer (Wescor 5600, Logan, UT, USA).

Hemolymph Cl^- analysis was determined by ion chromatography (Dionex ICS 2100, Sunnyvale, CA, USA). For measurements of Na^+ and K^+ concentrations, hemolymph (0.2 mL) was diluted and injected to an Inductively Coupled Plasma of Atomic Emission Spectroscopy technique (ICP-AES) (Optima 8000, Perkin Elmer, Boston, USA). The osmolality of the seawater was also measured following hemolymph sampling.

Fig. 1. Nucleotide and deduced amino acid sequence of *S. paramamosain* NKCC. The start and stop codons (asterisk) are in boldface. The polyadenylation signal (AATAAA) depicts in dotted line. A GT-repeat motif is underlined with bold line. The SLC12A domain (residues: 117-631) and the C-terminal tail domain (residues: 640-1053) are marked with wavy line and double-underline.

```
1     ACATGGGGAGGAACCATGAGCGCGGGGGAAGCAGATACTATTGAGTTGGACTCGGCGTCCCACATCCAAGTGGCCTCCGGGCTGGATGGC
1                     M  S  A  G  E  A  D  T  I  E  L  D  S  A  S  H  I  Q  V  A  S  G  L  D  G
91    ATGGACAGCCATCTCCACACCACGCACAGCCACTCCAACAGTGTGTACGAGACGCGCTACCAGAAGTCCCTGCGCCACTATCTGACCCGC
26     M  D  S  H  L  H  T  T  H  S  H  S  N  S  V  Y  E  T  R  Y  Q  K  S  L  R  H  Y  L  T  R
181   GAGGCGCTGCCCAAGGAGTCCCACTACAGGAATCTTGACTCTATCGTCGACGGATCTGCGCGCCCGACACTCGACGACCTGCACCACAAC
56     E  A  L  P  K  E  S  H  Y  R  N  L  D  S  I  V  D  G  S  A  R  P  T  L  D  D  L  H  H  N
271   ACGCTGAGGGAGAACCAGCGACAACAGGGGATAGACGCAGAAGCCGCCGCCGCCAACCCACGTGGCAAAGTTATCAAGTTCGGATGGCTG
86     T  L  R  E  N  Q  R  Q  Q  G  I  D  A  E  A  A  A  A  N  P  R  G  K  V  I  K  F  G  W  L
361   GAGGGAGTCTATATGCGATGCCTCCTCAACATCTGGGGCGTCATGTTGTTCCTCAGGGTGTCATGGGTGGTGGGCCAGTCTGGCATCATC
116    E  G  V  Y  M  R  C  L  L  N  I  W  G  V  M  L  F  L  R  V  S  W  V  V  G  Q  S  G  I  I
451   CTGGCACTCTTGACGGTGATCCTTGGAAACGTTGTCACCACTCTTACCACCTTGTCCATGTCTGCTGTGGCCACCAACGGGCGAATCCAA
146    L  A  L  L  T  V  I  L  G  N  V  V  T  T  L  T  T  L  S  M  S  A  V  A  T  N  G  R  I  Q
541   GCCGGTGGTGTCTACTACATGATCTCCCGCTCCCTTGGGCCTGAGTTTGGTGGCTCCATTGGGCTCATGTTCACCTTAGCTAACTCCATC
176    A  G  G  V  Y  Y  M  I  S  R  S  L  G  P  E  F  G  G  S  I  G  L  M  F  T  L  A  N  S  I
631   GCAGCTGCCACATATATCATTGGTTTCTGTGATTCCCTCCAGGATTTGATGTTCTTCTACTTTGATGGTGCTAAGATTGTGGACGGCGAA
206    A  A  A  T  Y  I  I  G  F  C  D  S  L  Q  D  L  M  F  F  Y  F  D  G  A  K  I  V  D  G  E
721   GTGAATGATACACGTATAGTGGGCACAATCACCCTCATATGTGTGCTGGCACTAGCCATTGTGGGCATGGATTGGGTCACCAGGGTCCAG
236    V  N  D  T  R  I  V  G  T  I  T  L  I  C  V  L  A  L  A  I  V  G  M  D  W  V  T  R  V  Q
811   ATGGGTTTGCTGTTCCTGCTGATTGGTTCACAGATTGACTTTGTGGTTGGTGCCTTCATTGGTCCCCAAAATGACCTGCAGAGGGCCCAG
266    M  G  L  L  F  L  L  I  G  S  Q  I  D  F  V  V  G  A  F  I  G  P  Q  N  D  L  Q  R  A  Q
901   GGCTTCATTGGCCTTAGCTCGGAGGTCATGGCCAAGAATGTCGGTCCGGATTATCGAGAGTTTGAGAATAGAGGACAGAACTTCTTCTCA
296    G  F  I  G  L  S  S  E  V  M  A  K  N  V  G  P  D  Y  R  E  F  E  N  R  G  Q  N  F  F  S
991   GTGTTCGGCGTGTTCTTCACCGCAGTGACGGGCATCGTGGCTGGGGCAAACCTTTCTGGAGATCTCAAGGACCCTGCAGAAGCTATCCCC
326    V  F  G  V  F  F  T  A  V  T  G  I  V  A  G  A  N  L  S  G  D  L  K  D  P  A  E  A  I  P
1081  AAAGGAACACTGGCAGCCATCTTAACCACCTTCTGCACCTACATCATCTACCCCATCATGATTGGAGCAGCCGTGCTGAGAGATGCCACA
356    K  G  T  L  A  A  I  L  T  T  F  C  T  Y  I  I  Y  P  I  M  I  G  A  A  V  L  R  D  A  T
1171  GGTGACAAAGATGTGTATGTGATGTACCAGAACCTCAGCATTGACGAAAATCCGGCATTCACAAATTGTAGCTTGATCGGCAAAGTTGAC
386    G  D  K  D  V  Y  V  M  Y  Q  N  L  S  I  D  E  N  P  A  F  T  N  C  S  L  I  G  K  V  D
1261  AATGGAACCCAAGTGTGTCCATTTGGCCTCCAGAACAGTTTTCAGGTGATGGAGCTCATGTCTGCCTGGGGACCTCTGATCTACGCTGGG
416    N  G  T  Q  V  C  P  F  G  L  Q  N  S  F  Q  V  M  E  L  M  S  A  W  G  P  L  I  Y  A  G
1351  TGCTTTGCTGCCACACTCTCCTCAGCCATTGCCTCCCTGGTGGGTGCCCCCAGGGTGCTGCAGGCGCTGGCCAAGGACAAACTCTATCCT
446    C  F  A  A  T  L  S  S  A  I  A  S  L  V  G  A  P  R  V  L  Q  A  L  A  K  D  K  L  Y  P
1441  GGCATCTTCATGTTCTCCAAGGGTACCGGTGCCAACAACGACCCTGTGCGTGGTTATGTCCTAGTCTTCGTCATCTCCTTTGTCTGCATC
476    G  I  F  M  F  S  K  G  T  G  A  N  N  D  P  V  R  G  Y  V  L  V  F  V  I  S  F  V  C  I
1531  ATGATTGGTGACCTGAACGTTGTCTCCACCCTGCTCAGTAACTTCTTCCTGGCATCGTACAGCCTCATCAACTTCTCCTGCTTCCATGCT
506    M  I  G  D  L  N  V  V  S  T  L  L  S  N  F  F  L  A  S  Y  S  L  I  N  F  S  C  F  H  A
1621  TCACTCATCAAGTCTCCTGGATGGCGGCCCAGTTTCAAGTATTACAACCTGTGGATCAGTTGGGTTGGTGGAATCTTGTGCCTGATTGTG
536    S  L  I  K  S  P  G  W  R  P  S  F  K  Y  Y  N  L  W  I  S  W  V  G  G  I  L  C  L  I  V
1711  ATGTTCTTAATTGACTGGGTTACCGCACTCATCACTTTCCTCATCACCGTCGCTCTCTACCTCTTTGTCCTACCGCAACCCCAATGTC
566    M  F  L  I  D  W  V  T  A  L  I  T  F  L  I  T  V  A  L  Y  L  F  V  S  Y  R  N  P  N  V
1801  AACTGGGGATCATCAACACAGGCACAGACTTATGTGTCGGCCCTCAAGACCACCCTGGACTTAAACAGCATCGAGGAGCATGTCAAGAAC
596    N  W  G  S  S  T  Q  A  Q  T  Y  V  S  A  L  K  T  T  L  D  L  N  S  I  E  E  H  V  K  N
1891  TACCGGCCACAGATTCTGGTGCTCAGTGGTCCTGTGGGCTCCAGGCCACCACTCATTGACTTTGCCTACAGCATCACCAAGAACATTTCC
626    Y  R  P  Q  I  L  V  L  S  G  P  V  G  S  R  P  P  L  I  D  F  A  Y  S  I  T  K  N  I  S
1981  CTGCTTGCCTGTGGTCATGTCATCCAGGGCCCCCAGACTCAGCGCCTGCGTAACTCCCTCACCCGGCAGTCTTACAACTGGCTTACCCGT
656    L  L  A  C  G  H  V  I  Q  G  P  Q  T  Q  R  L  R  N  S  L  T  R  Q  S  Y  N  W  L  T  R
2071  CACAGCATCCGTGCTTTCTACTCACTTGTGGAGGGGAGCAACTTAGAGGATGGTGCCAGAAACCTCTTCCAGCTTGTGGGTCTGGGTAAG
686    H  S  I  R  A  F  Y  S  L  V  E  G  S  N  L  E  D  G  A  R  N  L  F  Q  L  V  G  L  G  K
2161  CTGCGTCCCAACACTGTTGTCCTCGGCTACAAGGCAAACTGGCGCAAGTGTGACCCCTTGGAGCTCAAGGCATATTTCAACACCCTGCAT
716    L  R  P  N  T  V  V  L  G  Y  K  A  N  W  R  K  C  D  P  L  E  L  K  A  Y  F  N  T  L  H
2251  GAGGCTCTGGACATGTACTTTGGTGTGGTGATCCTCCGTGTGCCTCAGGGCCTGGACTACTCCCAGATCATTGAAGATGAGGACTCCCCC
746    E  A  L  D  M  Y  F  G  V  V  I  L  R  V  P  Q  G  L  D  Y  S  Q  I  I  E  D  E  D  S  P
2341  ATCACCATGAATGGCAATGAGAGTGCCATCACCCAGTCACCTGAAGATAAGCCAGGACAGTCCACTGCCAACCAGCTCACGCAAGATGGA
776    I  T  M  N  G  N  E  S  A  I  T  Q  S  P  E  D  K  P  G  Q  S  T  A  N  Q  L  T  Q  D  G
2431  ACAGACAGCGAGGCATCGAGTCCCCCAGGATCCCCTCAGGTAGAGCGCTCGGCAGCCACGACGGATGCCAACGGGGAGAACAGCAAGAAG
806    T  D  S  E  A  S  S  P  P  G  S  P  Q  V  E  R  S  A  A  T  T  D  A  N  G  E  N  S  K  K
2521  CGACGCACCTCCATGGCCAACTTGTTCCGAGGTCCAGGAGGTACCGAACTGAGCAAGGATGTCCTCAACAATATCACCATGTTCAAGAGG
836    R  R  T  S  M  A  N  L  F  R  G  P  G  G  T  E  L  S  K  D  V  L  N  N  I  T  M  F  K  R
2611  AAGCAGAAGAAGGGCACCATTGACGTGTGGTGGCTGTATGATGATGGTGGCCTGACGCTGCTGGTGCCCTACATCCTCACCACGCGCTCC
866    K  Q  K  K  G  T  I  D  V  W  W  L  Y  D  D  G  G  L  T  L  L  V  P  Y  I  L  T  T  R  S
2701  CAGTGGTCTGGGTGCAAGCTGAGAGTGTTCGCACTAGCCAATCGCAAGGATGAGCTGGACATGGAGCAGAGGAGCATGGCCAACCTGCTC
896    Q  W  S  G  C  K  L  R  V  F  A  L  A  N  R  K  D  E  L  D  M  E  Q  R  S  M  A  N  L  L
2791  GCCAAGTTCAGAATAGACTACAGCGATGTGATTGTCATCCCTGATGTGGCCAAGAAGGCTGCCGAGTCTTCCCGCATGGAGTTTGACCAG
926    A  K  F  R  I  D  Y  S  D  V  I  V  I  P  D  V  A  K  K  A  A  E  S  S  R  M  E  F  D  Q
2881  CTGATTGAGGACTTCAGGACCAAGGACGAGGTGGACAAGGAGAATGACGGACTCATGATCAGTGAGGCAGAGTTCCTGGGGCAGAGAGAG
956    L  I  E  D  F  R  T  K  D  E  V  D  K  E  N  D  G  L  M  I  S  E  A  E  F  L  G  Q  R  E
2971  AAGACTAATCGCCACATCCGTCTAAGGGAGTTGCTACTTGAAAACTCCAGAGATTCTTCCCTTGTCGTGATGACGCTGCCGATGCCCCGC
986    K  T  N  R  H  I  R  L  R  E  L  L  L  E  N  S  R  D  S  S  L  V  V  M  T  L  P  M  P  R
3061  AAGACGTCTGTGTCAGCCCCACTGTACATGGCCTGGCTGGAAACACTCACCCGCGACATGCCTCCCTTCCTCCTCATCCGCGGCAACCAA
1016   K  T  S  V  S  A  P  L  Y  M  A  W  L  E  T  L  T  R  D  M  P  P  F  L  L  I  R  G  N  Q
3151  ACCTCCGTTCTCACCTTCTACTCATAATGGACATATGTGAAATTTTTTTATTAGGATTTTAAGGTTCAAATGTGAATGAATGTTGCTGAT
1046   T  S  V  L  T  F  Y  S  *
3241  TGCTTTGTACAATAACAGTGTCTTTTACACGCAGAAAATTGTGTGTGTGAGTGTGTGTGTGTGTGTGTGTGTGTGTGTGTGTGTGT
3331  GTGTGTGTGTGTGTGTGTGTGAATGAGTGACTTTTAGAAATGAACTCTTTGGGATACGTTCATGCAACAGTTTTTAATTTTTTTTTATAA
3421  ATGCTTCATTAATACAAATATACAATATTTGTCATTAGTAGTATTAGCACAATTCTGTTTAAGCAAATTACTAGCGTTTCATTTTGTACA
3511  TTCCATGAGTGATGAGTGAGAAAGATCATATCATCTCATACTGTCTTCTGATTTCTCCAAAATACTCCCACAAAGATTCTTAATTACAAA
3601  AGTTTGACAATCTGAAGCACATATCAGACCAGATCAAGGCACAAAAAGTGAAATAATGACCAGTGTTATTTTTTAATGTGTATAAAAGTG
3691  TAGTTGATTTTGAATTGCCAATACTGTTAAGTTCCCAGGTGTGTTGGTGAACTGTGAGGCTCTGAACACCTGGCAGCGCGAACCATCATC
3781  CCATAGTTCAGTTTTGTTTGTAGTGAAGACACGTACTGAAATTGGAAAGTGGAACATGTATTCATACTTTTCGTAAACCTGAAACATTCC
3871  TTAATTGAAGAGTCGTGTAGTGGCATCAGTGCTCCCCACTCTCTGTTCATGGTCACAGTATTATACAACATGAATACAACAACTATCTCT
3961  TAATTGCCTGAAAATGGGAGAAAAATGTGTAAGGTATACAGTAAGTTGTAGCTTAATATCTTGTACATTGAAAGAGAATGAAAATTGGCA
4051  AATTGGAGGCAGACTGTAAAAGGTAAACAGGTAGTGATCAATTATATGCATTGCAATAAACCCAAAATAAAAAAAAAAAAAAAAAAAAA
4141  AAAAAAAAAAA
```

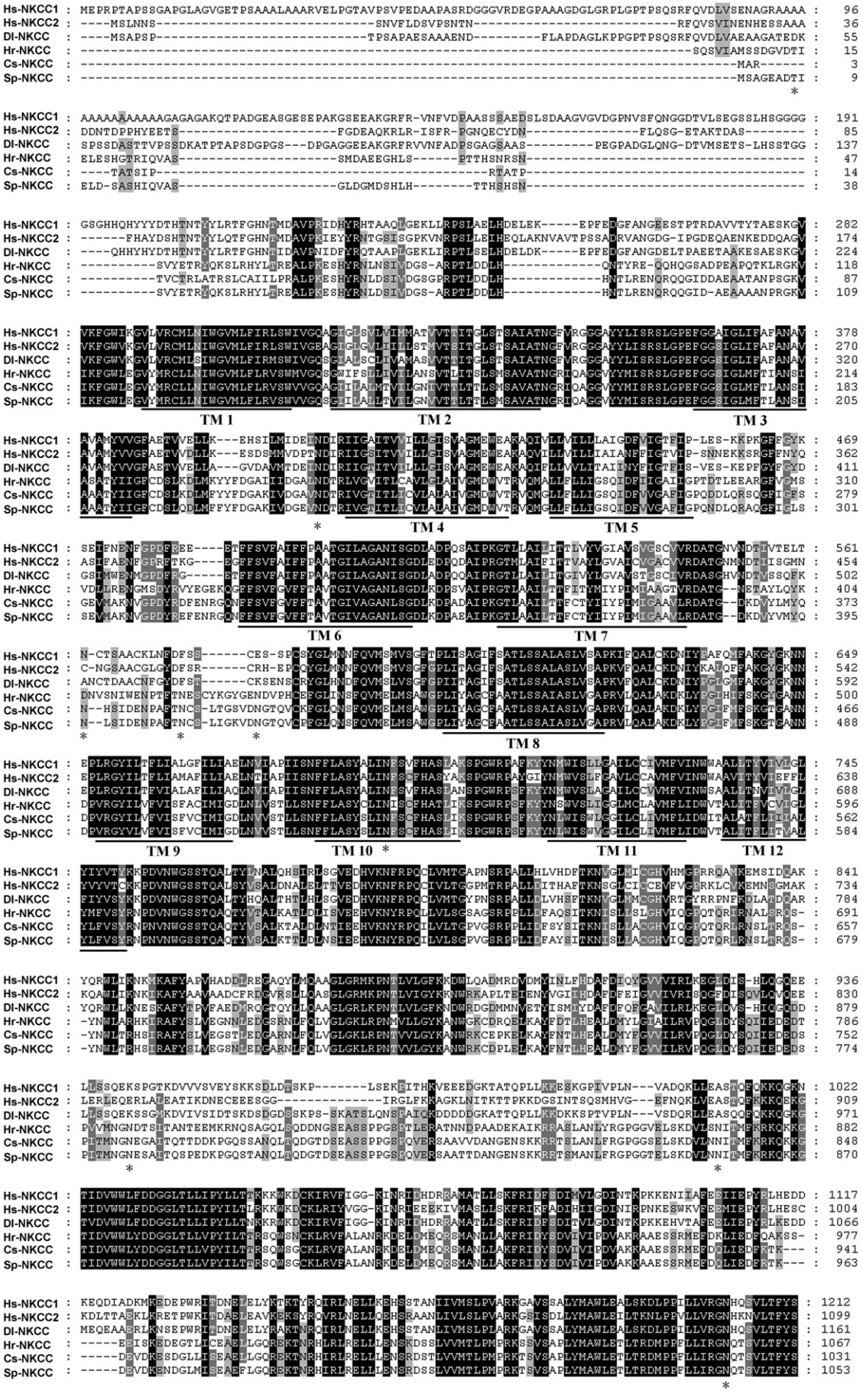
Hs-NKCC1
Hs-NKCC2
Dl-NKCC
Hr-NKCC
Cs-NKCC
Sp-NKCC
TM 1
TM 2
TM 3
TM 4
TM 5
TM 6
TM 7
TM 8
TM 9
TM 10
TM 11
TM 12

2.5. Cloning and sequencing of the branchial NKCC

2.5.1. cDNA fragments amplification

Total RNA was extracted from gills of *S. paramamosain* by using RNAiso Plus (TaKaRa, Dalian, China) according to the manufacturer's protocol. All RNA samples treated with gDNA Eraser were subjected to syntheses of cDNAs using PrimeScript® RT reagent Kit (TaKaRa, Dalian, China).

To obtain the cDNA fragment of *SpNKCC* (*S. paramamosain* NKCC), degenerate primers SpNKCC-F and SpNKCC-R (Table 1) were designed based on the homologies between published *NKCC* sequences. PCR for putative *SpNKCC* segments were performed and the PCR products were electrophoresed on an agarose gel, purified and cloned into a pMD19-T vector with a TA cloning kit (TaKaRa, Dalian, China). The recombinant plasmids were transformed into DH5α chemically competent cell of *Escherichia coli* (TaKaRa, Dalian, China). The positive clones were screened by PCR and then sequenced. Finally, the resulting sequences were verified and subjected to analysis in NCBI.

2.5.2. Rapid amplification of cDNA ends (RACE)

To synthesize first-strand cDNA for RACE reactions, 1 μg mRNA was reverse transcribed using reagents and a protocol provided in a SMARTer™ RACE cDNA Amplification Kit (Clontech, Palo Alto, CA, USA). Both the 3′-cDNA end and the 5′-cDNA end reaction conditions and components were performed according to the manufacturer's instructions. PCR products were isolated, purified, cloned, and sequenced as described in the cDNA fragment amplification. Primers were listed in Table 1.

2.6. Bioinformatics analysis

The full-length cDNA sequence was identified by BLAST analysis in NCBI database (http://www.ncbi.nlm.nih.gov). The predicted amino acid sequence was determined using the EXPASY molecular biology server (http://web.expasy.org/blast/). SpNKCC molecular mass and phosphorylation sites were predicted by ProtParam (http://web.expasy.org/protparam/) and NetPhos programs (http://www.cbs.dtu.dk/services/NetPhos/), respectively. Prediction of NKCC domain and features were performed using the InterPro Scan (http://www.ebi.ac.uk/interpro/scan.html). N-glycosylation sites were predicted at (http://www.cbs.dtu.dk/services/NetNGlyc/). Multiple alignments were performed using the ClustalX 1.81 software (http://www.clustal.org/) and edited by the GeneDoc software (http://www.psc.edu/biomed/genedoc/). The neighbor-joining tree estimated from distances between the animal NKCC amino acid sequences was built by Mega version 5.0 (http://www.megasoftware.net/), using P-distance and 1000 bootstrap (Tamura et al., 2011). Deduced protein sequences of NKCC from various species were retrieved from the GenBank (http://www.ncbi.nlm.nih.gov/genbank/).

2.7. Tissue distribution

Total RNA from the different tissues (gills, muscle, hepatopancreas, gut, thoracic ganglia, hypodermis, hemocytes, antennal gland and heart) of crabs (intermolt) was isolated to investigate the tissue distribution of *SpNKCC*. After cDNA was synthesized, quantitative real-time polymerase chain reaction (qPCR) were assayed for the levels of *SpNKCC* expression using an SYBR® Advantage® qPCR Premix (TaKaRa, Dalian, China) on an Applied Biosystems 7500 instrument (Applied Biosystems Carlsbad, CA).

SpNKCC real-F and SpNKCC real-R were used to generate *SpNKCC* fragment, while β-actin real-F and β-actin real-R were used to amplify corresponding *β-actin* fragment as the reference (Chung and Lin, 2006; Huang et al., 2012). All primers for the qPCR were ensured to produce a single PCR product of the predicted size and were quantified using the standard curve generated from serial dilutions (1, 0.1, 0.01, 0.001 and 0.0001 fold dilution series) of cDNA transcribed from gills mRNA. The real time PCR reaction was performed in triplicates in a final volume of 20 μL reaction mixture each (10 μL of SYBR Premix Ex Taq, 6.8 μL of water, 2 μL of cDNA, 0.4 μL of ROX and 0.4 μL of each primer). PCR conditions were as follows: 95 °C for 30 s; 40 cycles at 95 °C for 5 s and 60 °C for 30 s; and a melt from 60 to 95 °C. The relative expression level of *SpNKCC* was calculated by the comparative threshold cycle method ($2^{-\Delta\Delta Ct}$) (Livak and Schmittgen, 2001).

2.8. Histological and electron microscopic study

The anterior gills (Gills 1) and posterior gills (Gills 6) were dissected from 3 animals in intermolt stage. For the histology analysis, gills were incubated in 10% formaldehyde solution for 48 h, dehydrated in graded alcohol series, cleared with xylene and embedded in paraffin. Tissue sections (4 μm) were stained with hematoxylin–eosin (H&E) for general morphology and observed under a microscope (Nikon, Tokyo, Japan). Pictures were taken with 400 × magnification using a microscope digital camera (Toupcam, Hangzhou, China).

For transmission electron microscopy (TEM) study, specimens were fixed with 2.5% glutaraldehyde overnight. Following several short washings in 0.1 M sodium phosphate buffer (pH 7.0), the samples were fixed into 1% osmium tetroxide in the same buffer solution. After fixing, they were dehydrated in a graded series of ethanol and then absolute acetone. After dehydration, these samples were embedded in epoxy resin. Finally, thin sections about 80 nm were mounted on copper grids to be reviewed under electron microscope Hitachi Model H-7650 (Hitachi, Tokyo, Japan). Six pictures from different gill lamellae were taken from each animal using the same conditions.

2.9. Determination of SpNKCC transcript abundance during a molt cycle

To explore the possible involvement of *SpNKCC* in osmoregulation during the molt cycle, the expression of *SpNKCC* from posterior (G6) gills in different molt stages were determined using real-time PCR as described above.

2.10. Branchial gene expression of ion transporters and pumps; water channels during the molt cycle

To further investigate whether other previously identified genes also contribute to molt-related osmoregulation in *S. paramamosain* (Towle and Weihrauch, 2001; Luquet et al., 2005; Serrano et al., 2007), partial cDNA fragments of *NHE*, *CAc* and *AQP-1* were cloned with primers (Table 1) using the method described above. Subsequently, specific primers (Table 1) were designed for *S. paramamosain* targeting three genes:

NKA α, *CAc* and *NHE*. The mRNA expression of the *NKA α* was studied using specific primers designed according to *NKA α*-subunit sequence from the *S. paramamosain* gill (Chung and Lin, 2006). Because of its role in water transport, the gene expression of AQP-1 protein was also measured (Aoki et al., 2003; Martinez et al., 2005; Giffard-Mena et al., 2007; Raldúa et al., 2008). All the expression profiles of these genes from the posterior (G6) gills in different molt stages were determined by qPCR as described above.

Fig. 2. Alignment of the deduced amino acid sequences of multiple NKCC proteins. Sequences and accession numbers are shown for the following: *S. paramamosain* (NKCC, **KT923171**), *Callinectes sadus* (NKCC, **AAF05702**), *Halocaridina rubra* (NKCC, **AIM43576.1**), *Dicentrarchus labrax* (NKCC1, **ABB84251.1**), *Homo sapiens* (NKCC1, **NP 001037.1**), *Homo sapiens* (NKCC2, **NP 000329**). Underlined and labeled are twelve predicted transmembrane domains (TM1-TM12). Potential N-linked glycosylation sites (bold N, positions 237, 396, 407, 416, 529, 653, 781 and 1044) are highlighted in asterisk.

2.11. Statistical analysis

The data were subjected to statistical analysis by a one-way ANOVA followed by Tukey's multiple comparisons or unpaired Student *t*-test when appropriate using Prism 5.0 (Graph-Pad, La Jolla, CA). The observed differences were considered significant at $P < 0.05$. All data were presented as means ± standard error (SEM) of triplicate measurements on each of seven separate preparations.

3. Results

3.1. cDNA cloning and sequence analysis of SpNKCC

A full-length cDNA (4151 base pairs) corresponding to a *NKCC* gene of *Scylla paramamosain* (GenBank accession no. **KT923171**) was obtained by RT-PCR coupled to RACE-PCR. The nucleotide and deduced amino acid sequence are shown in Fig. 1. The corresponding gene was designated as *SpNKCC*. It is composed of a 15-bp 5′-untranslated region (UTR), a 3162-bp open reading frame (ORF) and a 974-bp 3′-UTR. The open reading frame encodes a 1053 amino acid protein. A GT-repeat motif is located 824 bp upstream of the polyadenylation signal (AATA AA) in the 3′-UTR region (Fig. 1). The deduced protein has a predicted molecular mass of about 116.5 kDa and a theoretical pI of 6.08. It consists of a SLC12A domain (residues 117-631) of 414 amino acid residues followed by 12 transmembrane domains and a hydrophilic cytoplasmic C-terminal tail (residues 640-1053) (Fig. 1). In addition, the protein has 8 putative N-linked glycosylation sites (Fig. 2, bold N at positions 237, 396, 407, 416, 529, 653, 781 and 1044) and 51 potential phosphorylation sites (31 serine, 12 threonine and 8 tyrosine), respectively (Fig. 1).

Multiple protein sequence alignment analysis is shown in Fig. 2. Although the similarity of this gene was low compared to vertebrates NKCCs (63.70%–65.88%), the SpNKCC revealed high similarity to other decapoda NKCC from crustaceans (87.28%–97.22%). A phylogenetic analysis of the NKCC protein sequences revealed the expected relationship between *S. paramamosain* and other species (Fig. 3). Accordingly, NKCCs can be divided into two subclasses: vertebrate NKCCs (NKCC1 and NKCC2) and invertebrate NKCC. In the invertebrates, SpNKCC was clustered with blue crab *Callinectes sapidus* NKCC and allocated to be a member of crustacean NKCC.

3.2. Tissue distribution of SpNKCC

The expression of *SpNKCC* was expressed in all tissues examined (Fig. 4), including gills, muscle, hepatopancreas, gut, thoracic ganglia, hypodermis, hemocytes, antennal gland and heart. The highest expression level of *SpNKCC* was found in gills, while the lowest was in heart (ANOVA, $P < 0.05$, Fig. 4A). Among the individual gills (Fig. 4B), the relative abundance of the *SpNKCC* transcript was expressed in all 8 gills (*S. paramamosain* has 8 pairs of gills, Supplementary File 1) and the expression of *SpNKCC* in posterior gills (G6–G8) was about 5 to 10-fold higher than that in anterior gills (ANOVA, $P < 0.05$, Fig. 4B).

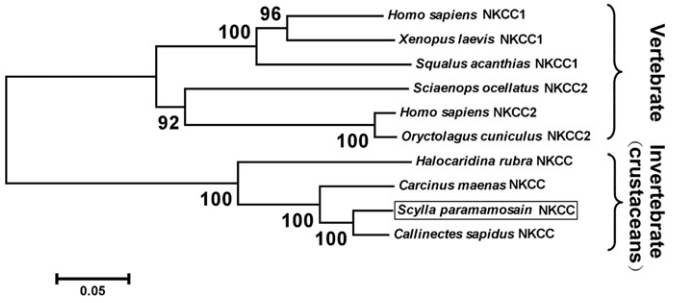

Fig. 3. Phylogenetic analysis of the amino acid sequences of NKCC. The genetic distance was built by the Neighbor-Joining Method with 1000 bootstrap replicates. The GenBank numbers are as follows: *Homo sapiens* (NKCC1, **NP 001037.1**; NKCC2, **NP 000329**), *Xenopus laevis* (NKCC1, **NP 001091331.1**), *Squalus acanthias* (NKCC1, **P55013.1**), *Sciaenops ocellatus* (NKCC2, **AIL54060.1**), *Oryctolagus cuniculus* (NKCC2, **P55015**), *Halocaridina rubra* (NKCC, **AIM43576.1**), *Carcinus maenas* (NKCC, **AAK62044.1**), *S. paramamosain* (NKCC, **KT923171**), *Callinectes sapidus* (NKCC, **AAF05702**).

3.3. Structure of the gill epithelia

The structure of anterior and posterior gills lamellae from *S. paramamosain* were examined (Fig. 5). In each gill lamella of *S. paramamosain*, two symmetrical single-layered epithelia facing each other across the hemolymph space occasionally occupied by a central intralamellar septum and mechanically sustained by the pillar cells (Fig. 5A). Each lamella was covered by thin cuticle (Fig. 5B).

Ultrastructural differences were noted when comparing the lamellae in posterior and anterior gills. In the anterior gills, the epithelium was dominated by thin cells, associated with a few mitochondria in the basolateral side and moderate surface amplification in the apical region (Fig. 5B). In contrast, thick cells in posterior gills exhibited abundant mitochondria, conspicuous basolateral infoldings and extensive apical folds (Fig. 5B). Moreover, the hematoxylin–eosin staining results showed that a wide circulatory space was more evident between thin epithelial layers in the anterior gills (Fig. 5A).

3.4. Changes in hemolymph osmolality and ionic concentrations at different stages of the molt cycle

Hemolymph osmolality varied during the molt cycle (Fig. 6A). The lowest level of hemolymph osmolality was approximately 549 ± 19 mOsm kg^{-1} at the postmolt stage A. This level increased significantly to 713 ± 4 mOsm kg^{-1} at stage B (ANOVA, $P < 0.05$), followed by an increasing trend from intermolt to premolt (stage C-D_2, ANOVA, $P < 0.05$) and reached a maximum level at stage D_2 (802 ± 8 mOsm kg^{-1}). The osmolality level in stage E was then determined to be 758 ± 3 mOsm kg^{-1}. Overall, hemolymph osmolality in *S. paramamosain* was approximately 73–337 mOsm kg^{-1} above that in the sea water (476 ± 1 mOsm kg^{-1}) (Fig. 6A), confirming that *S. paramamosain* is a relatively strong osmoregulator.

Fluctuations in Na^+, Cl^-, K^+ in the hemolymph of the *S. paramamosain* during the molt cycle were examined. Na^+ concentrations in the hemolymph increased significantly from stage A (236.1 ± 7.4 mmol L^{-1}) to stage C (376.3 ± 5.1 mmol L^{-1}) (ANOVA, $P < 0.05$, Fig. 6B). The Na^+ level reached 411.9 ± 4.3 mmol L^{-1} at stage D_2, and dropped to 304.7 ± 11.0 mmol L^{-1} at ecdysis (ANOVA, $P < 0.05$, Fig. 6B). Fluctuations in chloride (Cl^-) hemolymph concentrations showed a pattern similar to those of hemolymph osmolality and Na^+ concentrations (Fig. 6C). Following ecdysis (stage A, 266.0 ± 18.5 mmol L^{-1}), concentrations increased rapidly (ANOVA, $P < 0.05$) at the postmolt stage B (325.0 ± 9.2 mmol L^{-1}) and reached 361.6 ± 4.3 mmol L^{-1} at the intermolt stage. Thereafter, the Cl^- level was relatively constant (ANOVA, $P > 0.05$) from premolt D_0 to D_2 (ranging 366.0 ± 9.9 mmol L^{-1} to 400.1 ± 16.2 mmol L^{-1}). At molting, level presented a value of 368.9 ± 13.6 mmol L^{-1}. K^+ concentrations in the hemolymph during a full molt cycle are presented in Fig. 6D. In general, there were no statistically significant changes in K^+ content in all the stages with the exception of the stage E (other stages, ranging 8.7 ± 0.9 mmol L^{-1} to 11.6 ± 0.8 mmol L^{-1}; stage E, 8.1 ± 1.1 mmol L^{-1}), where a decrease was observed (ANOVA, $P < 0.05$).

3.5. Growth performance

To explain the hemolymph osmolality and ionic concentrations variation following ecdysis, the increment of size and weight resulting from molting is reported in Fig. 7. Overall percentage increase in weight was 106.13% (Student's *t*-test, $P < 0.05$, Fig. 7A). Meanwhile, the carapace width was increased from 47.1 ± 0.3 mm to 62.8 ± 0.3 mm, while

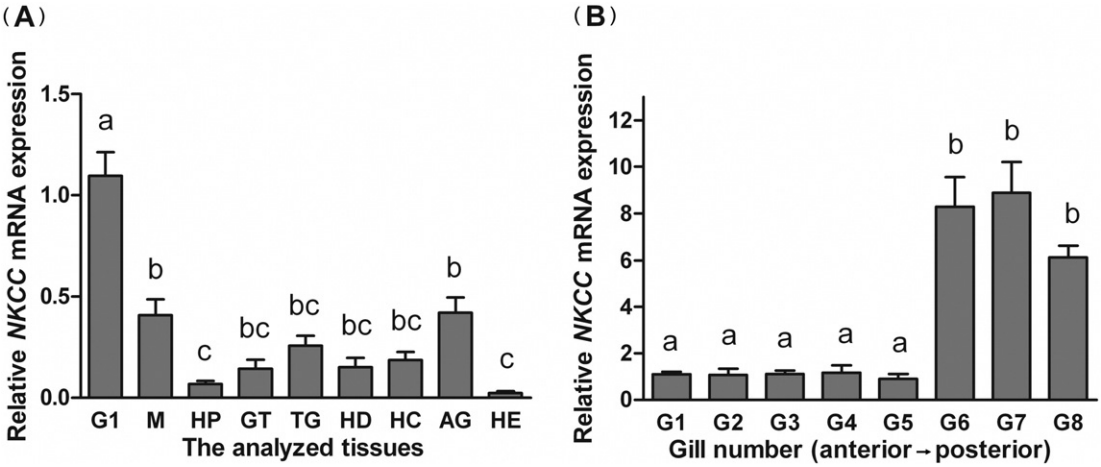

Fig. 4. Expression of *SpNKCC* in the tissues obtained from juvenile crabs at intermolt stage. The tissue distribution of *SpNKCC* in crab is shown relative to expression in gill 1. (A) *SpNKCC* transcript levels in crab tissues: G1 = gill 1, M = muscle, HP = hepatopancreas, GT = gut, TG = thoracic ganglion, HD = hypodermis, HC = hemocytes, AG = antennal gland and HE = heart. (B) Expression of *SpNKCC* in gills 1–8. G1–G8, individual gills from the anterior to the posterior of the crab. Vertical bars represent the mean ± SEM, $n = 7$. Means with different superscript letters are significantly different (one-way ANOVA, Tukey's multiple comparisons test, $P < 0.05$).

the carapace length was increased from 34.1 ± 0.2 mm to 42.5 ± 0.1 mm (Student's *t*-test, $P < 0.05$, Fig. 7A), respectively.

3.6. Expression of SpNKCC in posterior gills during molt cycle

To gain some insight into the potential role of *SpNKCC* during the molt cycle, the expression level of its gene was quantified by qPCR in posterior gills at various molt stages (Fig. 8). The expression was lowest in molt (used as calibrator). This transcript then attained a high expression level at early premolt (stage A, 26.7-fold, ANOVA, $P < 0.05$). It significantly elevated at late premolt (stage B, 338.8 -fold, ANOVA, $P < 0.05$) and then decreased during the following intermolt and premolt stages (stage C-D_2).

3.7. Branchial gene expression of NKA α, NHE, CAc and AQP-1 during the molt cycle

To characterize differences in iono-regulatory mechanisms in the posterior gills of *S. paramamosain* at different molt stages, we examined

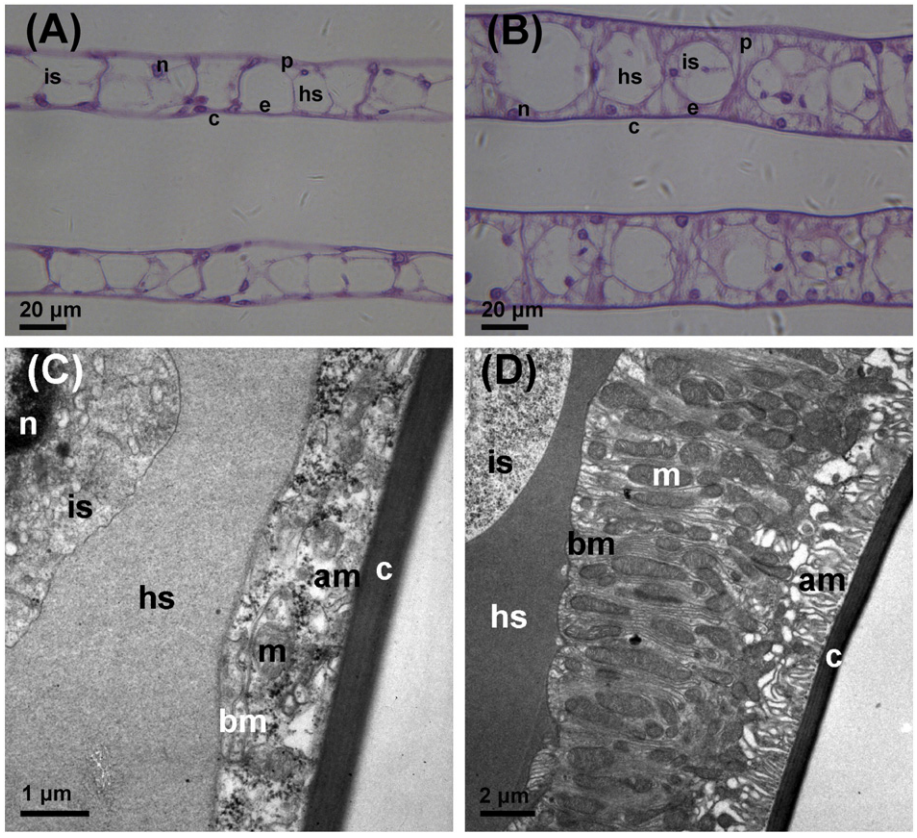

Fig. 5. Structures of epithelial cells in posterior (A–C) and anterior gill (B–D) of *S. paramamosain* (intermolt). Photomicrographs of semi-thin sections of gill 1 (A) and 6 (B) lamellae stained with hematoxylin-eosin (H & E). Both images are 400 ×. (C) Ultrastructure of respiratory-type cell in anterior gill epithelium of the *S. paramamosain*. (D) Ultrastructure of ion-transporting-type cell in posterior gill epithelium of the *S. paramamosain*. am: apical membrane; bm: basal membrane; c: cuticle; e: epithelial cell; hs: hemolymph space; is: intralamellar septum; m: mitochondrion; n: nucleus; p: pillar cell. Scale bar in (A) and (B), 20 μm; in (C), 1 μm and (D), 2 μm.

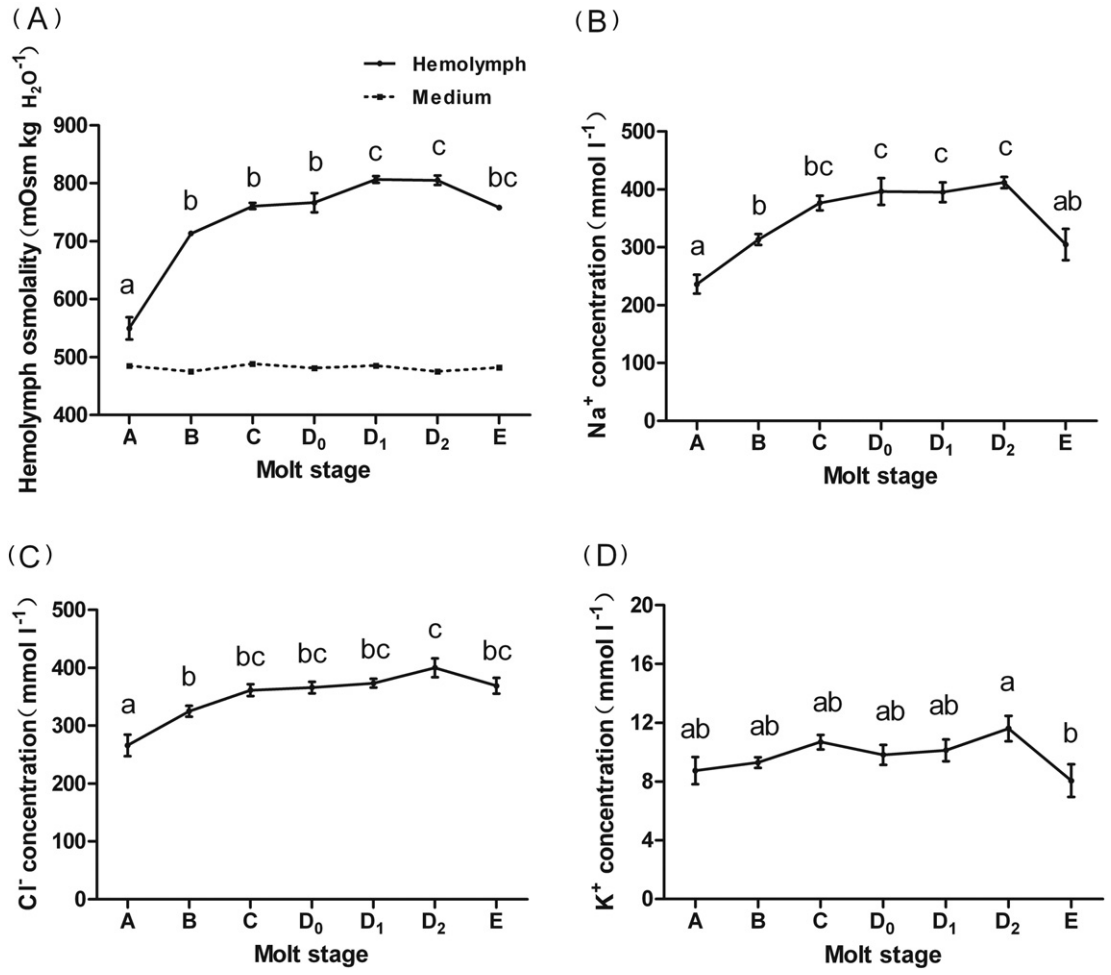

Fig. 6. Changes in hemolymph osmolality and ion concentrations in *S. paramamosain* during the molt cycle. (A) Osmolality, (B) Na^+ concentrations, (C) Cl^- concentrations and (D) K^+ concentrations. The molt stages are defined based on the established criteria (Drach and Tchernigovtzeff, 1967). Results are shown as the mean ± SEM, n = 7. Means with different superscript letters are significantly different (one-way ANOVA, Tukey's multiple comparisons test, $P < 0.05$).

gene expression of key ion transporting proteins and water channel previously characterized in other euryhaline crabs (Fig. 9). Homologs of *NHE*, *CAc* (osmoregulatory isoform) and *AQP-1* were identified from the *S. paramamosain* gills (Supplementary File 2), and GenBank accession numbers are **KU317606**, **KU317607** and **KX247397**, respectively.

The patterns of expression of mRNA abundance for the *NKA* α (Fig. 9A), *CAc* and *NHE* were similar to that for *NKCC*. Following ecdysis, *NKA* α mRNA in posterior gills increased 9.5-fold at stage A over the level in animals at stage E (ANOVA, $P < 0.05$), and elevated at stage B (41.7-fold, ANOVA, $P < 0.05$), then fell sharply at intermolt and premolt (ANOVA, $P < 0.05$). In posterior gills, the level of *CAc* transcript (Fig. 9B) was lowest in molting crabs, and it increased about 21.4-fold to a peak in postmolt stage B (ANOVA, $P < 0.05$). It was then gradually decreased to the similar level of that at stage A (ANOVA, $P < 0.05$). Similarly, *NHE* transcription in posterior gills (Fig. 9C) was significantly raised in the postmolt stage B (79.9-fold, ANOVA, $P < 0.05$), then followed by a decreasing trend from intermolt to premolt.

The pattern of *AQP-1* mRNA expression over the molt cycle was, however, different from that of NKCC gene expression (Fig. 9D). The expression level of *AQP-1* mRNA in posterior gills was low during the intermolt and premolt and then increased 3.8-fold at the molting stage E (ANOVA, $P < 0.05$), and remained high during the postmolt (stage A–B).

4. Discussion

Data presented in the current study provide the first information on the full length sequence of the *NKCC* derived from the gills of *S. paramamosain* (Fig. 1). Phylogenetic analysis of the SpNKCC confirmed its similarity to crustacean NKCC (Fig. 3). We know from previous studies that vertebrates NKCC duplicated in two major isoforms: a basolateral isoform (NKCC1), involved in NaCl excretion and an apical form (NKCC2), involved in NaCl uptake (Markadieu and Delpire, 2014). However, the resulting sequence information was insufficient to classify the product as apical or basolateral. Whether a second NKCC isoform exists in the crustacean genome as it found in vertebrates warrants further investigation.

Structurally, the deduced SpNKCC contains all signature domains of the Na^+-dependent subgroup of solute carrier 12 (SLC12) family of transporters, including a SLC12A domain, 12 transmembrane domains, intracellular N- and C-termini domain (Fig. 1) that is important for maturation, dimerization, and protein trafficking to the plasma membrane (Markadieu and Delpire, 2014). Previous studies have shown that NKCCs may be activated by direct phosphorylation in the NH_2-terminus during osmotic stress (Lytle and Forbush, 1992; Giménez and Forbush, 2005). The presence of numerous potential phosphorylation sites in the NH_2-terminus of the *S. paramamosain* might be involved in the up-regulation of NKCC. All NKCCs are glycoproteins (Lytle and Forbush, 1992; Arroyo et al., 2013) which possess sites for N-linked glycosylation within a large hydrophilic loop between putative TM7 and TM8 (Payne and Forbush, 1995), and the consensus sites for N-linked glycosylation had been identified in the NKCC of *S. paramamosain*. The glycosylation in the large TM7-TM8 loop was considered crucial for transport activity, membrane expression, and affinity for loop diuretics (Paredes et al., 2006).

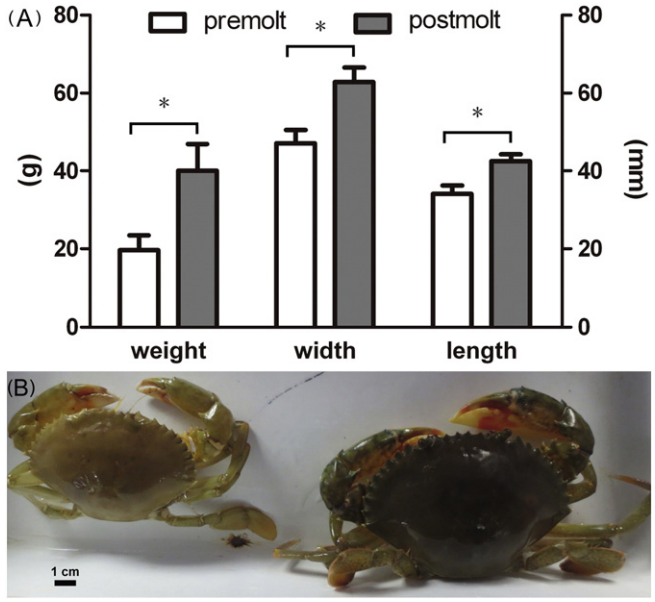

Fig. 7. Molt-induced growth change in *S. paramamosain* from premolt stage D_2 to postmolt stage A. (A) Changes in body weight, width and length in *S. paramamosain* from stage D_2 to stage A. (B) Detail showing the molting in *S. paramamosain*, the crab on the right has just molted; its old exoskeleton is on left. The molt stages are defined based on the established criteria (Drach and Tchernigovtzeff, 1967). Scale bars: 1 cm. Asterisks on top of the columns indicate significant differences from the premolt control stage (*t*-test with $P < 0.05$).

The profile of *SpNKCC* expression in tissues showed that the *SpNKCC* transcript was highest in the posterior gills with a broad lower level expression of this transporter across many tissues (Fig. 4). The posterior gills of euryhaline crabs are believed to be particularly specialized for ion transport on the basis of high expression of the ion transport protein (Towle et al., 1997a). Given the direct correspondence between posterior gills and ion transport across multiple crustacean species, the expression of *SpNKCC* in the posterior gills may function as likely.

The gill ultrastructure of *S. paramamosain* verifies our interpretation of the *SpNKCC* gene expression pattern among different gills (Fig. 5). Generally, the gills ultrastructure of *S. paramamosain* corroborates the

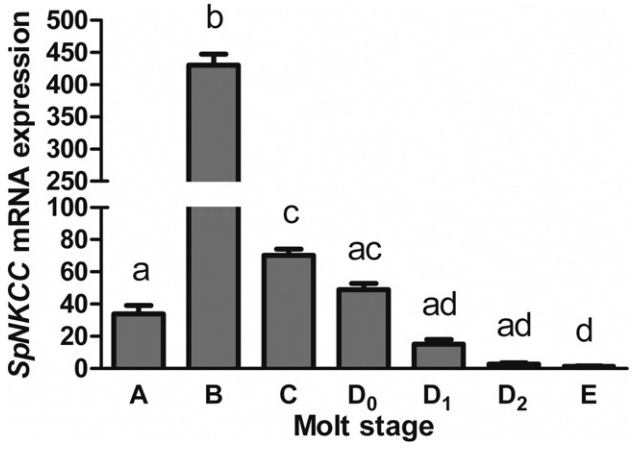

Fig. 8. Quantitative real-time PCR (qPCR) assays of *SpNKCC* expression in the gills of *S. paramamosain* at various molt stages. Molting stages are depicted as follows: postmolt (A–B); intermolt (C); early premolt (D_0) mid premolt (D_1); late premolt (D_2) and molting (E). *SpNKCC* transcript levels were normalized to that of *S. paramamosain* at ecdysis. The molt stages are defined based on the established criteria (Drach and Tchernigovtzeff, 1967). Values are expressed as means ± SEM, n = 7. Means with different superscript letters are significantly different (one-way ANOVA, Tukey's multiple comparisons test, $P < 0.05$).

previous descriptions of the currently accepted phyllobranchiate gill model (Towle and Weihrauch, 2001; Freire et al., 2008), where ion transport mechanisms seem to be located in functionally different gills. The posterior gills have a number of distinct ultrastructural features that are characteristic of ion transporting epithelia. These include abundant mitochondria in the sub-apical cytoplasm, a greatly elaborated membrane surface (particularly in the basolateral region facing hemolymph space), and extensive foldings in the apical surface of the leaflets. The dense membrane foldings network presents a large surface area for the insertion of transport proteins such as the vacuolar-type ATPase (V-ATPase) and the NKA (Boudour-Boucheker et al., 2014). Numerous mitochondria may provide the ATP and related phosphagens that power active transport processes (Towle and Weihrauch, 2001). Compared to posterior gills, the anterior gills that are believed to play roles in both respiration and acid–base regulation are equipped with relatively larger hemolymph space, much thinner epithelial cells with limited membrane elaboration, and a few mitochondria (Goodman and Cavey, 1990; Freire et al., 2008). Thus, the fact that *SpNKCC* mRNA expression was higher in posterior gills than that in anterior gills suggests that branchial NKCC is more important for ion regulation in posterior gills.

This investigation has revealed remarkable changes in osmolality, Na^+ and Cl^- levels in the hemolymph of *S. paramamosain* at different stages of the molt cycle (Fig. 6). This was attributed to discontinuous growth pattern in crustaceans during the molt cycle. Similar results were observed in *C. maenas* (Robertson, 1960), *Macrobrachium rosenbergii* (Wilder et al., 2009) and *Litopenaeus vannamei* (Jasmani et al., 2010). At ecdysis, the *S. paramamosain* allowed water (106.13%-fold of weight) to be absorbed to facilitate withdrawal from the carapace (Fig. 7), which leads to a dramatically decrease in osmolality, Na^+ and Cl^- levels in the hemolymph after ecdysis (Fig. 6). Immediately preceding ecdysis, the rapid increase of Na^+ and Cl^- concentrations in the hemolymph indicated that osmotic balance was achieved through predominantly with ion absorbed from seawater. In premolt stages, the resultant higher osmotic gradient in the hemolymph might contribute to the rate of passive water uptake in low salinity environments at ecdysis. In contrast, the K^+ level was relatively constant during the molt cycle but was lower only at molting (Fig. 6D). Similar result was reported in *M. rosenbergii* (Wilder et al., 2009). Our measurement of the steady state K^+ level in the hemolymph of *S. paramamosain* indicated that a powerful mechanism underlying K^+ uptake might be involved in K^+ homeostasis regulation during the molt cycle.

This study also presents data on the pattern of the expression of *SpNKCC* during the molt cycle that link to its specific osmoregulatory role in the posterior gills (Fig. 8). According to the current hypothetical model for coupled Na^+ and Cl^- transport across the gill epithelium in estuarine brachyuran hyperosmoregulators, the NKCC would transport one Na^+, one K^+, and two Cl^- ions across the apical membrane (McNamara and Faria, 2012). The increase in *SpNKCC* mRNA parallels the increase in osmolality, Na^+ and Cl^- levels in animals from early postmolt to late postmolt (stage A, 26.7-fold; stage B, 338.8-fold) suggests that an absorptive form may be induced at postmolt stages, where it could function in the absorption of the ions from the seawater. Similarly, *NKCC* expression was greater in the premolt stages when compared to molting stage (stage E), suggesting that it could function in maintaining higher rate of NaCl uptake from the medium. Several studies have found *NKCC* expression to be greater in the gills of crustacean transferred to lower salinity (Spanings-Pierrot and Towle, 2004; Luquet et al., 2005; Havird et al., 2014). Moreover, a dependence of Cl^- absorption on K^+ was demonstrated in the split gill lamellae of the shore crab *C. maenas* (Riestenpatt et al., 1996). Therefore, these observations would imply a potential role for NKCC in absorption of ions from the medium. However, the study in *C. granulatus* showed that the *NKCC* was upregulated following higher and lower salinity seawater transfer, revealing dependence on NKCC-driven ion uptake and salt secretion in euryhaline crab (Luquet et al., 2005). It therefore appears that a complex

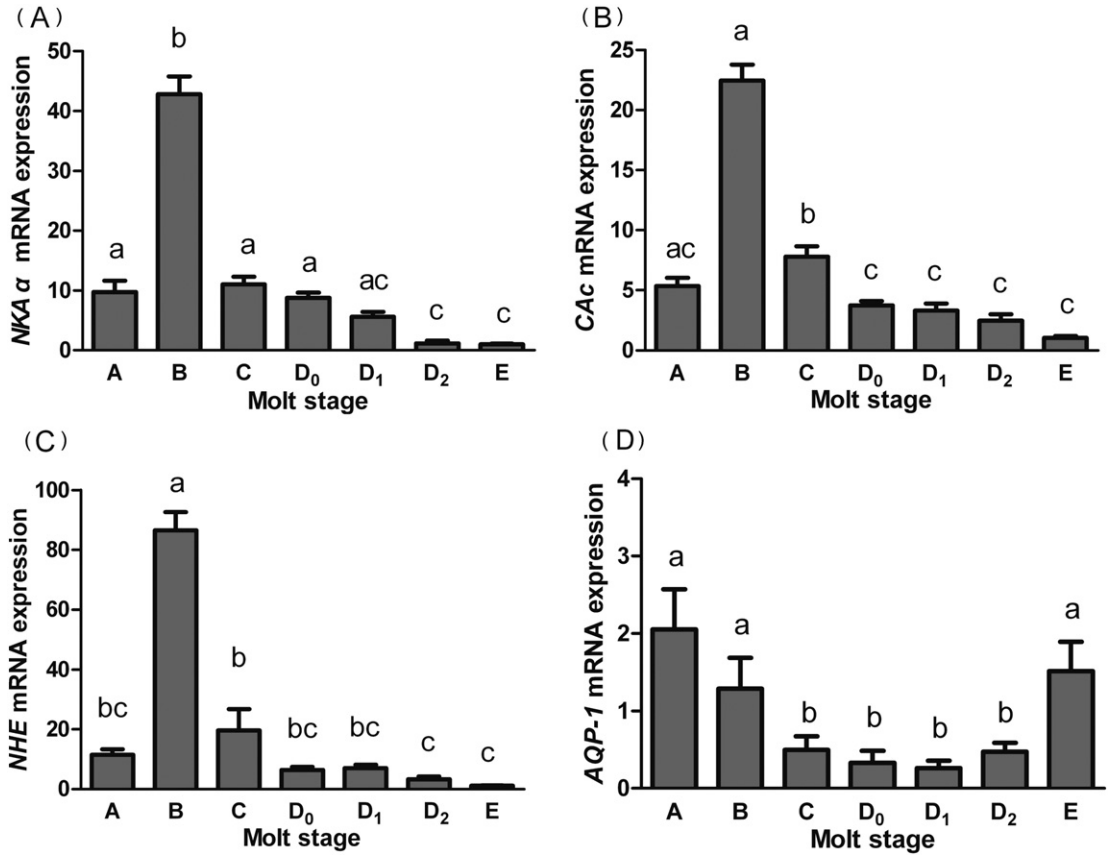

Fig. 9. *NKA α* (A), *NHE* (B), *CAc* (C) and *AQP-1*(D) mRNA levels in posterior gills of *S. paramamosain* during the molt cycle. The molt stages are defined based on the established criteria (Drach and Tchernigovtzeff, 1967). Values are expressed as means ± SEM, n = 7. Means with different superscript letters are significantly different (one-way ANOVA, Tukey's multiple comparisons test, $P < 0.05$).

regulatory mechanism of NKCC might exist in crustaceans. Future establishing the adequate NKCC antibody specific for decapod transporters could provide a useful tool to ascertain its physiological role in ion regulation.

Consistent with their roles in ions uptake, *NKA α*, *CAg*, *NHE* showed the similar pattern of gene expression as *SpNKCC* (Fig. 9). The dynamic changes in gene transcripts involved in branchial osmoregulation observed in the current experiment provide evidence that regulation of ions uptake in different molt stages involves a coordinated suite of changes in osmoregulatory genes. Adjusting levels of gene expression can be rapid in postmolt stages, with the largest degree of inductive scope occurring within the first 2–3 days after ecdysis, typically the same time period in which hemolymph osmotic and ionic concentrations stabilize at new, regular levels. The largest increase in *NKAα* and *CAc* expression was observed at postmolt stage following ecdysis in the gills of *S. paramamosain*, perhaps therefore providing driving force and enhancing the supply of counterions for NaCl uptake respectively as outlined above. Increased *NKA α* and *CAc* transcription would increase the pool of NKA α and CAc protein. For example, in the blue crab *C. sapidus*, elevated activity of NKA during postmolt was observed (Towle and Mangum, 1985). In parallel, NHE, has been considered as a candidate in the uptake of Na^+ by gills of euryhaline crabs living in low salinities (Towle and Weihrauch, 2001; McNamara and Faria, 2012). Although the localization of NHE have not yet been explored in crustacean gills, the higher expression levels of *NHE* in the posterior gills of *C. maenas* than that in the anterior gills may therefore indicate a role of this antiporter in osmoregulation as previously suggested for fish (Choe et al., 2005; Scott et al., 2005; Kumai and Perry, 2012). Moreover, a recent study in our lab have shown that the relative abundance of *NHE* mRNA in the posterior gills of *S. paramamosain* was increased significantly after transfer from 28 to 5 ppt (Xu et al., unpublished). This suggests that NHE may play a role in NaCl uptake when crabs are resident in low salinity. In this study, the increased expression of *NHE* (10.5 to 79.9-fold) in the gills during the ion uptake stages may provide more compelling support for a role of NHE in Na^+/H^+ exchange during the postmolt stages.

The aquaporin (AQP) family of water channels, small and very hydrophobic intrinsic membrane proteins, has been identified to potentially play roles in water and solute transport (Borgnia et al., 1999). In marine fish, the AQP-1 has been shown to be vital for absorption of imbibed water across the cell membrane by up-regulating its mRNA expression (Aoki et al., 2003; Martinez et al., 2005; Giffard-Mena et al., 2007; Raldúa et al., 2008). In contrast, the involvement of aquaporins in water transport has been rarely studied in crustacean. Gao et al. (2009) demonstrated the relative mRNA expression of *AQP* in antennal gland was lower in the premolt when compared to the intermolt and postmolt stages. Additionally, the *AQP-1* expression of *C. sapidus* differed with ontogeny during larval development, with significantly higher expression at early larval stages in the exposure of hyposalinity (Chung et al., 2012). In this study, the expression of *AQP-1* in the posterior gills was significantly increased from molting to postmolt (Fig. 9D). Given the visible changes in uptake of water around ecdysis and elimination of water load in postmolt, the higher expression of *AQP-1* in gills of *S. paramamosain* may be responsible for water absorption at molting to aid in the exuviation process.

In summary, the present study identified a full length ortholog of the $Na^+/K^+/2Cl^-$ cotransporter, *SpNKCC*, in *S. paramamosain*. The *SpNKCC* transcript was abundantly expressed in ion-regulating gills. Expression of *SpNKCC* and a coordinated suite of genes increased in gills of *S. paramamosain* in the postmolt stages when ion uptake rate was demonstrated to increase significantly. This suggests that *SpNKCC* may

implicate its involvement in the ion uptake of *S. paramamosain* in the postmolt stages.

Supplementary data to this article can be found online at http://dx.doi.org/10.1016/j.cbpa.2016.08.019.

Acknowledgements

This work was funded by Zhejiang Provincial Key Project of Science and Technology Research (No. 2015C02054), Zhejiang Provincial Key Project of Aquaculture Breeding (No. 2016).

References

Aoki, M., Kaneko, T., Katoh, F., Hasegawa, S., Tsutsui, N., Aida, K., 2003. Intestinal water absorption through aquaporin 1 expressed in the apical membrane of mucosal epithelial cells in seawater-adapted Japanese eel. J. Exp. Biol. 206, 3495–3505.

Arroyo, J.P., Kahle, K.T., Gamba, G., 2013. The SLC12 family of electroneutral cation-coupled chloride cotransporters. Mol. Asp. Med. 34, 288–298.

Borgnia, M., Nielsen, S., Engel, A., Agre, P., 1999. Cellular and molecular biology of the aquaporin. Annu. Rev. Biochem. 68, 425–458.

Boudour-Boucheker, N., Boulo, V., Charmantier-Daures, M., Grousset, E., Anger, K., Charmantier, G., Lorin-Nebel, C., 2014. Differential distribution of V-type H^+-ATPase and Na^+/K^+-ATPase in the branchial chamber of the palaemonid shrimp *Macrobrachium amazonicum*. Cell Tissue Res. 357, 195–206.

Chang, Y.J., Sun, C.L., Chen, Y., Yeh, S.Z., 2011. Modelling the growth of crustacean species. Rev. Fish Biol. Fish. 22, 157–187.

Choe, K.P., Kato, A., Hirose, S., Plata, C., Sindic, A., Romero, M.F., Claiborne, J.B., Evans, D.H., 2005. NHE3 in an ancestral vertebrate: primary sequence, distribution, localization, and function in gills. Am. J. Physiol. Regul. Integr. Comp. Physiol. 289, 1520–1534.

Chung, K.F., Lin, H.C., 2006. Osmoregulation and Na^+/K^+-ATPase expression in osmoregulatory organs of *Scylla paramamosain*. Biochem. Physiol. A 144, 48–57.

Chung, J.S., Maurer, L., Bratcher, M., 2012. Cloning of aquaporin-1 of the blue crab, *Callinectes sapidus*: its expression during the larval development in hyposalinity. Aquat. Biosyst. 8, 21.

Drach, P., Tchernigovtzeff, C., 1967. Sur la méthode de détermination des stades d'intermue et son application générale aux crustacés (in French with English abstract). Vie Milieu Ser. A 18, 595–609.

Freire, C.A., Onken, H., McNamara, J.C., 2008. A structure-function analysis of ion transport in crustacean gills and excretory organs. Biochem. Physiol. A 151, 272–304.

Gagnon, E., Forbush, B., Caron, L., Isenring, P., 2002. Functional comparison of renal $Na^+/K^+/2Cl^-$ cotransporters between distant species. Am. J. Physiol. Cell Physiol. 284, 365–370.

Gamba, G., 2005. Molecular physiology and pathophysiology of electroneutral cation-chloride cotransporters. Physiol. Rev. 85, 423–493.

Gao, Y., Gao, Y.P., Wheatly, M., Krane, C., 2009. Cloning and expression of aquaporin in the antennal gland of crayfish, *Procambarus clarkii*. FASEB J. 23, 998.6.

Ghanawi, J., Saoud, I.P., 2012. Molting, reproductive biology, and hatchery management of redclaw crayfish *Cherax quadricarinatus* (von Martens 1868). Aquaculture 358, 183–195.

Giffard-Mena, I., Boulo, V., Aujoulat, F., Fowden, H., Castille, R., Charmantier, G., Cramb, G., 2007. Aquaporin molecular characterization in the sea-bass (*Dicentrarchus labrax*): the effect of salinity on AQP-1 and AQP-3 expression. Comp. Biochem. Physiol. A Mol. Integr. Physiol. 148, 430–444.

Giménez, I., Forbush, B., 2005. Regulatory phosphorylation sites in the NH_2 terminus of the renal $Na^+/K^+/2Cl^-$ cotransporter (NKCC2). Am. J. Physiol. Ren. Physiol. 289, 1341–1345.

Goodman, S.H., Cavey, M.J., 1990. Organization of a phyllobranchiate gill from the green shore crab *Carcinus maenas* (Crustacea, Decapoda). Cell Tissue Res. 260, 495–505.

Havird, J.C., Santos, S.R., Henry, R.P., 2014. Osmoregulation in the Hawaiian anchialine shrimp *Halocaridina rubra* (Crustacea: Atyidae): expression of ion transporters, mitochondria-rich cell proliferation and hemolymph osmolality during salinity transfers. J. Exp. Biol. 217, 2309–2320.

Henry, R.P., 1988. Multiple functions of gill carbonic anhydrase. J. Exp. Zool. 248, 19–24.

Huang, J.R., Huang, H.Y., Ye, H.H., 2012. Cloning and analysis of beta-actin gene from *Scylla paramamosain*. J. Xiamen Univ. 51, 274–279 (in Chinese with English abstract).

Jasmani, S., Jayasankar, V., Shinji, J., Wilder, M.N., 2010. Carbonic anhydrase and Na^+/K^+-ATPase activities during the molt cycle of low salinity-reared white shrimp *Litopenaeus vannamei*. Fish. Sci. 76, 219–225.

Kumai, Y., Perry, S.F., 2012. Mechanisms and regulation of Na^+ uptake by freshwater fish. Respir. Physiol. Neurobiol. 184, 249–256.

Leone, F.A., Garcon, D.P., Lucena, M.N., Faleiros, R.O., Azevedo, S.V., Pinto, M.R., McNamara, J.C., 2015. Gill-specific Na^+/K^+-ATPase activity and α-subunit mRNA expression during low-salinity acclimation of the ornate blue crab *Callinectes ornatus* (Decapoda, Brachyura). Comp. Biochem. Physiol. B 186, 59–67.

Li, X., Xu, Z., Zhou, G., Lin, H., Zhou, J., Zeng, Q., Mao, Z., Gu, X., 2015. Molecular characterization and expression analysis of five chitinases associated with molting in the Chinese mitten crab, *Eriocheir sinensis*. Biochem. Physiol. B 187, 110–120.

Livak, K.J., Schmittgen, T.D., 2001. Analysis of relative gene expression data using real-time quantitative PCR and the 2(T)(−Delta Delta C) method. Methods 25, 402–408.

Luquet, C.M., Weihrauch, D., Senek, M., Towle, D.W., 2005. Induction of branchial ion transporter mRNA expression during acclimation to salinity change in the euryhaline crab *Chasmagnathus granulatus*. J. Exp. Biol. 208, 3627–3636.

Lytle, C., Forbush, B., 1992. The $Na^+/K^+/2Cl^-$ cotransporter protein of shark rectal gland. 2. Regulation by direct phosphorylation. J. Biol. Chem. 267, 25438–25443.

Markadieu, N., Delpire, E., 2014. Physiology and pathophysiology of SLC12A1/2 transporters. Pflugers Arch. - Eur. J. Physiol. 466, 91–105.

Martinez, A.S., Cutler, C.P., Wilson, G.D., Phillips, C., Hazon, N., Cramb, G., 2005. Cloning and expression of three aquaporin homologues from the European eel (*Anguilla anguilla*): effects of seawater acclimation and cortisol treatment on renal expression. Biol. Cell. 97, 615–627.

McNamara, J.C., Faria, S.C., 2012. Evolution of osmoregulatory patterns and gill ion transport mechanisms in the decapod Crustacea: a review. J. Comp. Physiol. B. 182, 997–1014.

Ong, K.S., 1966. Observations on the post-larval life history of *Scylla serrata* reared in the laboratory. Malays. Agric. J. 45, 429–445.

Paredes, A., Plata, C., Rivera, M., Moreno, E., Vazquez, N., Munoz-Clares, R., Hebert, S.C., Gamba, G., 2006. Activity of the renal $Na^+/K^+/2Cl^-$ cotransporter is reduced by mutagenesis of N-glycosylation sites: role for protein surface charge in Cl^- transport. Am. J. Physiol. Ren. Physiol. 290, 1094–1102.

Payne, J.A., Forbush, B., 1995. Molecular characterization of the epithelial $Na^+/K^+/2Cl^-$ cotransporter isoforms. Curr. Opin. Cell Biol. 7, 493–503.

Perry, H., Trigg, C., Larsen, K., Freeman, J., Erickson, M., Henry, R., 2001. Calcium concentration in seawater and exoskeletal calcification in the blue crab, *Callinectes sapidus*. Aquaculture 198, 197–208.

Raldúa, D., Otero, D., Fabra, M., Cerdá, J., 2008. Differential localization and regulation of two aquaporin-1 homologs in the intestinal epithelia of the marine teleost *Sparus aurata*. Am. J. Physiol. Regul. Integr. Comp. Physiol. 294, 993–1003.

Riestenpatt, S., Onken, H., Siebers, D., 1996. Active absorption of Na^+ and Cl^- across the gill epithelium of the shore crab *Carcinus maenas*: voltage-clamp and ion-flux studies. J. Exp. Biol. 199, 1545–1554.

Robertson, J.D., 1960. Osmotic and ionic regulation. In: Waterman, T.H. (Ed.), The Physiology of Crustaceans vol. 1. Academic Press, New York, pp. 317–339.

Scott, G.R., Claiborne, J.B., Edwards, S.L., Schulte, P.M., Wood, C.M., 2005. Gene expression after freshwater transfer in gills and opercular epithelia of killifish: insight into divergent mechanisms of ion transport. J. Exp. Biol. 208, 2719–2729.

Serrano, L., Henry, R.P., 2008. Differential expression and induction of two carbonic anhydrase isoforms in the gills of the euryhaline green crab, *Carcinus maenas*, in response to low salinity. Biochem. Physiol. D 3, 186–193.

Serrano, L., Halanych, K.M., Henry, R.P., 2007. Salinity-stimulated changes in expression and activity of two carbonic anhydrase isoforms in the blue crab *Callinectes sapidus*. J. Exp. Biol. 210, 2320–2332.

Spanings-Pierrot, C., Towle, D.W., 2004. Salinity-related mRNA expression of the $Na^+/K^+/2Cl^-$ cotransporter and V-type H^+-ATPase in gills of the euryhaline crab *Pachygrapsus marmoratus*. Bull. Mt. Desert Isl. Biol. Lab. 43, 6–8.

Tamura, K., Peterson, D., Peterson, N., Stecher, G., Nei, M., Kumar, S., 2011. MEGA5: molecular evolutionary genetics analysis using maximum likelihood, evolutionary distance, and maximum parsimony methods. Mol. Biol. Evol. 28, 2731–2739.

Towle, D.W., Mangum, C.P., 1985. Ionic regulation and transport atpase activities during the molt cycle in the blue crab *Callinectes sapidus*. J. Crustac. Biol. 5, 216–222.

Towle, D.W., Weihrauch, D., 2001. Osmoregulation by gills of euryhaline crabs: molecular analysis of transporters. Am. Zool. 41, 770–780.

Towle, D.W., Rushton, M.E., Heidysch, D., Magnani, J.J., Rose, M.J., Amstutz, A., Jordan, M.K., Shearer, D.W., Wu, W.S., 1997a. Sodium/proton antiporter in the euryhaline crab *Carcinus maenas*: molecular cloning, expression and tissue distribution. J. Exp. Biol. 200, 1003–1014.

Towle, D.W., Weihrauch, D., Fooks, A., Cohen, Z.S., 1997b. Molecular identification and cDNA sequencing of a $Na^+/K^+/2Cl^-$ cotransporter in gills of the euryhaline blue crab *Callinectes sapidus*. Am. Zool. 37, 87A.

Wilder, M.N., Huong, D.T.T., Jasmani, S., Jayasankar, V., Kaneko, T., Aida, K., Hatta, T., Nemoto, S., Wigginton, A., 2009. Hemolymph osmolality, ion concentrations and calcium in the structural organization of the cuticle of the giant freshwater prawn *Macrobrachium rosenbergii*: changes with the molt cycle. Aquaculture 292, 104–110.

Xu, B.P., Tu, D.D., Shu, M.A., 2016. Identification and expression of an Na^+ / H^+ exchanger (NHE) in the gills of the euryhaline mud crab, *Scylla paramamosain*, in response to low salinity seawater, unpublished.

Xu, B.P., Long, C., Dong, W.R., Shao, Q.J., Shu, M.A., 2015. Molecular characterization of calreticulin gene in mud crab *Scylla paramamosain*: implications for the regulation of calcium homeostasis during molt cycle. Aquac. Res. http://dx.doi.org/10.1111/are.12781.